International Journal of Design & Nature and Ecodynamics
Vol. 17, No. 5, October, 2022, pp. 639-648
Journal homepage: http://iieta.org/journals/ijdne

# Dissolved Oxygen Variation on the Steps with a Quarter Circle End Sill for Flows over the Stepped Spillways

Udai A. Jahad[1], Riyadh Al-Ameri[2], Ali Chabuk[1], Ali Majdi[3], Hasan Sh. Majdi[3], Nadhir Al-Ansari[4*], Jan Laue[4]

[1] Department of Environment Engineering, College of Engineering, University of Babylon, Babylon 51001, Iraq
[2] School of Engineering, Deakin University, 75 Pigdons Road, Waurn Ponds, VIC 3220, Australia
[3] Al-Mustaqbal University College, Babylon 51001, Iraq
[4] Department of Civil Environmental and Natural Resources Engineering, Lulea University of Technology, SE-971 87 Lulea, Sweden

Corresponding Author Email: alansari@ltu.se

https://doi.org/10.18280/ijdne.170501

**Received:** 18 June 2022
**Accepted:** 8 August 2022

***Keywords:***
*flow, dissolved, oxygen, stepped, spillway*

**ABSTRACT**

Determining the aeration efficiency of the stepped spillways is important because the Dissolved Oxygen (DO) concentration helps indicate the water quality. This study investigated the effects of varying step shape and chute slope on the aeration efficiency for stepped spillways. The measured parameters were DO, the inception point of the free surface, and the water surface profile above the crest to evaluate the geometry variation impacts. Several experiments were conducted on a six-step configuration over a stepped spillway with chute angle (θ = 26.6°, 21.8°, and 8.9°). The discharges up to 0.055 $m^3/s$. The step configurations were including flat step, normal end sill, and quarter circle end sill. The results showed when the chute angle changed from 26.6° to 8.9°, the aeration efficiency of E20 improved with 11.51% at the lowest discharge and 6.05% at the highest discharge for the flat step model with 10 steps. Also, E20 improved 11.39% at the lowest discharge and 6.50% at the highest discharge for the flat step model with 6 steps. The performance of the steps with the quarter circle end sill model in terms of aeration efficiency increased by 10%.

## 1. INTRODUCTION

Aeration is a process for the mass transfer of air between the atmosphere and water. It is used to improve the water quality in sewage treatment plants and polluted rivers and lakes [1]. Moreover, the gas transfer is a significant component of water quality in white water. The poor quality of the water may have decreased oxygen concentration. Also, it means increasing the nitrogen, chlorine, and volatile organic compound concentrations, or methane from the decomposition of organic matter. The most significant parameter that refers to water quality is the dissolved oxygen (DO) content [2].

The flow of gases, for example, oxygen, in the interface between air and water, can be assessed as follows:

$$\frac{dC}{dt} = k_L \frac{A}{\forall}(C_s\text{-}C) \quad (1)$$

where, dc/dt: is the rate of change in concentration; A: is the surface area of bubbles; ∀: is the volume of water in which C and A are measured and C: is DO concentration in water; $C_S$: is saturation concentration of oxygen in water; $k_L$: is the liquid film coefficient, and t: is the time.

The factors affecting oxygen transfer in Stepped spillways are water temperature, water quality, the depth of tailwater, drop height, weir discharge, and the DO deficit upstream [3].

The flow over hydraulic structures such as stepped spillways improve the aeration process and transfer of oxygen. The concentration of DO has been increased by using a stepped spillway. Air entrainment in spillways is used in wastewater treatment plants, fish hatcheries, and rivers. The stepped spillway is a series of steps that generate this process that flows into the face of the chute in a stepped spillway. Stepped spillways structures can be designed as clarifiers and for re-aeration. Stepped spillways may be utilized to improve the process of aeration in the treatment of plants and rivers [4]. There are previous researchers that studied the geometry effect on the aeration process (e.g., Wang et al. [5], Ashour et al. [6], and Felder et al. [7]).

Studies demonstrate how energy dissipation and DO can be affected by stepped spillway geometry. The air entrainment depends on the inception point location for the flow over the stepped spillway. The location of the inception point can be affected by discharges, step geometry, and step configuration [8]. The parameters have been examined for an internal air-water flow in a smooth channel with a length of 25 m and a slope of 4°.

The study determined the length of the chord for air bubbles and the frequency of air bubbles by using a probe of 25 μm tip diameter scanning at 40 kHz with double-tip conductivity. Additionally, the flow of mixed air-water has homogeneous concentrations for air (C: DO concentration in water) lower than 0.9. The two regions for air-water occur: (i) the first one is a bubbly flow region when C < 0.3 - 0.4, and (ii) a highly aerated flow region when C > 0.3 - 0.4. The results illustrate that the frequency profiles for non-dimensional air bubbles are a high value [9]. In another hand, the effect of channel slope on aeration efficiency has been explained in stepped spillways. The study demonstrated that the aeration efficiency of stepped

spillway aerators increases with increasing channel slope [10]. The study showed the relation between aeration efficiency and the energy dissipation over stepped spillways. From the results, it is noted that the aeration efficiency increases with increasing the energy dissipation rate. The energy dissipation in the nappe flow regime is greater than in the skimming flow regime. Also, the nappe flow regime leads to higher aeration efficiency than the skimming flow regime [11]. The stepped spillway is an effective structure regarding the energy dissipation and the re-aeration processes. Overall, it was clear that spillway geometry (e.g., slope, and height of micro-roughness) affected the velocity and depth of flow. Furthermore, the parameters were important for oxygen transfer because they affected the process of air entrainment, and that lead to an effect on the size and the amount of entrained air bubbles. The size and amount of entrained air bubbles depended on the air-water interface. The used scale of the physical models was 1:10 for a stepped spillway and varied the height of the steps and the angle of the chute. The discharges are conducted with objective analyses of the development of the flow properties in the non-uniform flow region. A double-tip conductivity probe was used to measure the velocity of the mixture (air-water) and the concentration of the air. In the step, the macro-roughness has a different effect on the flow characteristics [12]. Spillways with rounded edge steps were examined experimentally to compare with the flat steps. The flow is recognized and introduced as a transition to the skimming flow. The skimming flow on rounded steps was achieved faster than with the flat steps. Loss of energy rate was increased by 3% with rounded stepped spillways. The study noted that the inception length was increased for rounded spillways transferring small discharges that lead to more stability inflow and faster change to skimming flow. In rounded edge spillways, the length of the air-water mixture increased with high discharges (high velocities), such that the risk of cavitation damage was reduced. They found that the height of the training wall was low and had more inception depth in a rounded-edge spillway. The height of the training wall in a rounded-edge spillway was about 20% lower than in sharp spillways. They recommended using steps with rounded edges for initial transition steps or the main spillway steps because they work better than flat step designs [13].

The characteristics of air-water flow in a flat pooled stepped waterway have been investigated. The study was done on a large-size facility of dimensions, and the intrusive probe had double-tip phase detection. The shapes used in that experimental work (flat horizontal steps, pooled steps, and a combination of flat and pooled steps). The properties of air-water flow for different flow rates were noted regularly. The outcomes contained data on flow resistance, energy dissipation, and the distribution of basic properties for air-water flow. Researchers found that pooled stepped spillways with a flat slope and θ = 8.9° allowed a larger energy dissipation rate than flat stepped spillways, and unstable flow can occur [14, 15].

This study aims to investigate the stepped spillway geometry effects regarding the dissolved oxygen (DO) and the inspection point location with Froude number (Fr) by using a new shape for the end sill (quarter circle end sill).

## 2. METHODOLOGY

### 2.1 Aeration efficiency

The aeration efficiency (E) can be defined mathematically by Eq. (2), assuming the saturation concentration of Cs is constant concerning time [16].

$$E = \frac{C_d - C_u}{C_s - C_u} \quad (2)$$

where, $C_u$ is the dissolved oxygen concentration upstream of the hydraulic structure and $C_d$ is the dissolved oxygen concentration downstream of the hydraulic structure.

The temperature has an impact on aeration efficiency. Usually, researchers have used a correction factor for temperature. Eq. (3) explains the relationship:

$$E\ 20 = 1 - (1 - E)^{(1/ft)} \quad (3)$$

where, E is the actual aeration efficiency; E20 is the aeration efficiency at 20°C and ft is the exponent described by Eq. (4) [16]:

$$ft = 1.0 + 0.02103(T - 20) + 8.261 \times 10^{-5} (T - 20)^2 \quad (4)$$

where, T = water temperature.

**Table 1.** Model's details of the experimental parameters tested

| Model | θ (°) | W (m) | hs (m) | ls (m) | End sill type | End sill height (m) | Ns | yc/hs |
|---|---|---|---|---|---|---|---|---|
| M1-1 | 26.6 | 0.5 | 0.03 | 0.067 | - | - | 10 | 0.66- 1.05 |
| M1-2 | | | 0.03 | 0.067 | normal | 0.03 | 10 | |
| M1-3 | | | 0.03 | 0.067 | quarter circle | 0.03 | 10 | |
| M1-4 | | | 0.05 | 0.120 | - | - | 6 | 0.69- 1.08 |
| M1-5 | | | 0.05 | 0.120 | normal | 0.05 | 6 | |
| M1-6 | | | 0.05 | 0.120 | quarter circle | 0.05 | 6 | |
| M2-1 | 21.8 | 0.5 | 0.03 | 0.083 | - | - | 10 | 0.66- 1.05 |
| M2-2 | | | 0.03 | 0.083 | normal | 0.03 | 10 | |
| M2-3 | | | 0.03 | 0.083 | quarter circle | 0.03 | 10 | |
| M2-4 | | | 0.05 | 0.150 | - | - | 6 | 0.69- 1.08 |
| M2-5 | | | 0.05 | 0.150 | normal | 0.05 | 6 | |
| M2-6 | | | 0.05 | 0.150 | quarter circle | 0.05 | 6 | |
| M3-1 | 8.9 | 0.5 | 0.03 | 0.210 | - | - | 10 | 0.66- 1.05 |
| M3-2 | | | 0.03 | 0.210 | normal | 0.03 | 10 | |
| M3-3 | | | 0.03 | 0.210 | quarter circle | 0.03 | 10 | |
| M3-4 | | | 0.05 | 0.380 | - | - | 6 | 0.69- 1.08 |
| M3-5 | | | 0.05 | 0.380 | normal | 0.05 | 6 | |
| M3-6 | | | 0.05 | 0.380 | quarter circle | 0.05 | 6 | |

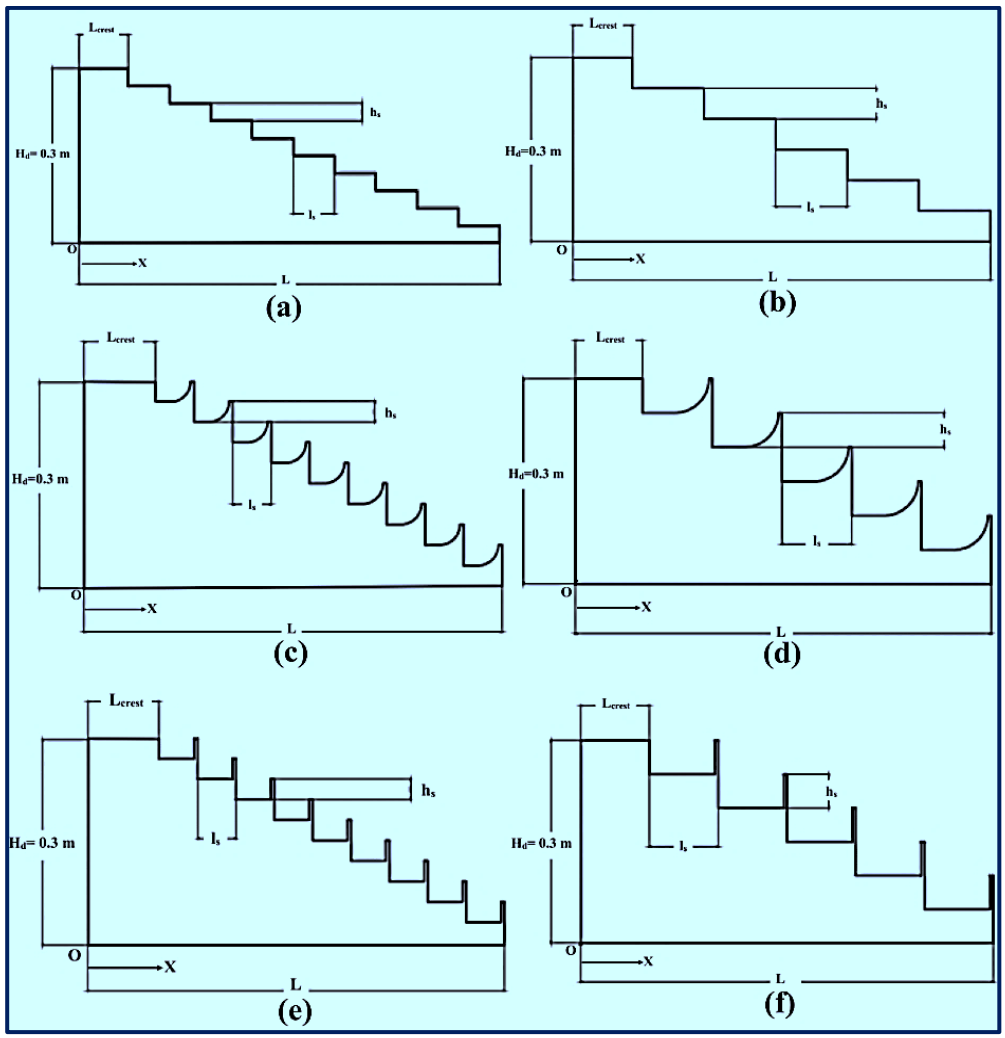


**Figure 1.** Stepped spillways with different shapes and dimensions tested. (a) Mi-1, (b) Mi-4, (c) Mi-2, (d) Mi-5, (e) Mi-5 and (f) Mi-6. where: i = 1, 2, and 3 for θ = 26.6°, 21.8°, and 8.9° respectively

### 2.2 Materials and procedure

The experimental work was conducted in a flume at Deakin University. The dimensions of the flume were 0.5 m in width, 0.6 m in depth, and 7.0 m in length. The discharge range was between (0.0045 $m^3/s$ to 0.055 $m^3/s$). The discharge was measured by the flow meter installed in the water supply pipe with an accuracy of ± 0.001 m3/s. The water was supplied by a pipe (diameter = 0.2 m) to the inlet tank and there was a matrix of pipes (diameter = 0.025 m) at this tank to get smooth and uniform flow before the test section. Three chute angels (θ = 26.6°, 21.8°, and 8.9°) were used in both the experimental and numerical approaches to team aeration efficiency. The weir depth was $H_d$ = 0.3 m with four-step configurations as shown in Table 1 and Figure 1. In the current study, tap water was utilized in the experiments and the water was changed at each experiment. Ideally, 7.9 $g/m^3$ of sodium sulphite is needed to eliminate 1 $g/m^3$ of DO. The estimated sodium sulphite that needs to be used is about 10-20% of the excess, and that is based on the tap water test for DO [17]. The sodium sulphite method was applied to deoxygenate the water in the tank. From the chemical calculations, the theoretical amount of sodium sulphite ($Na_2SO_3$) was approximately 70 gm required to deoxygenate 1 $m^3$ of water as shown in chemical Eq. (5).

$$2\ NaSO_3 + O_2 \rightarrow 2\ NaSO_4 \qquad (5)$$

In this study, the sodium sulphite was 70 gm + (10% to 15%) and that depends on the estimated DO of the test tap water with cobalt II chloride ($COCl_2$) 3.3 $g/m^3$. In general, the content of the salt in the tap water in this study was low and monitored during the experiment to ensure no effect on the residues caused by the deoxygenation chemicals added to the tap water. All the experiments were started by filling the tank with tap water and adding $Na_2SO_3$ with $COCl_2$ for the deoxygenation process. The Do was measured by using a calibrated portable WTW model oxi320 oxygen meters. Do concentrations were measured upstream and downstream of the spillway. The DO meters were calibrated daily by the calibration method recommended by the manufacturer. The aeration efficiency was corrected to the reference temperature (20°C) by using Eqns. (3) & (4) to prepare a basis for the comparison between the measured data. The non-aerated flow region length Li (for 0.45 < yc/hs < 1.6) can be calculated by Eq. (6) as below:

$$\frac{L_i}{hs\ cos\ \theta} = 1.05 + 5.11 \times \frac{q}{\sqrt{g\ sin\ \theta\ (hs \cos\theta)^3}} \qquad (6)$$

For flat steps spillway, Ks=hs cos θ and for pooled steps spillway, Ks = (hs + ws) cos θ.
where, ks is the step cavity height, ws is the sill height. Froude number F* defined in terms of the step cavity roughness [14]:

$$F* \frac{q}{\sqrt{g \sin\theta \; j \; k_s^3}} \quad (7)$$

## 3. RESULTS AND DISCUSSION

### 3.1 Experimental results

It is significant to find out the aeration efficiency on the stepped spillways to evaluate the water quality. The values for aeration efficiency were calculated from the difference between the upstream dissolved oxygen concentration Cu and the downstream Cd as shown in Eq. (2). In the current study, the aeration efficiency E20, where the investigated as a function of the chute angle (θ), step height (hs) and shape, discharge, and roughness Froude number (Fr*) [18].

There are three flow regimes (Nappe flow, Transition flow, and Skimming flow) that can be overstepped weirs depending on the discharge value. To find the flow regimes for flat stepped spillways for $0.05 < ls/hs < 1.7$ and $3.4° < \theta < 60°$), the upper and lower limits for Nappe flow and Skimming flow regimes, respectively are [19]:

$$\frac{y_c}{h_s} = 0.89 - 0.4 \times \frac{h_s}{l_s} \quad (8)$$

$$\frac{y_c}{h_s} = 1.2 - 0.325 \times \frac{h_s}{l_s} \quad (9)$$

where, the yc is the critical flow depth, hs and ls are the step height and step length respectively.

Figure 2 shows the flow regimes observations and their corresponding values yc/hs for the flat step Models with Eqns. (8) & (9) and results from other studies. It can be stated that the upper limit of the nappe flow regime was slightly less than Eq. (8), and the lower limit of the skimming flow regime was slightly more than Eq. (9). In general, the flow regimes in this study are consistent with the limits proposed by Eqns. (8) & (9) since the step geometry and chute angle are like the other studies. Within the range of parameters listed in Table 1 at least, this implies that variations in step configuration and θ have a significant impact on the flow regime, which is primarily governed by q, especially at low flow.

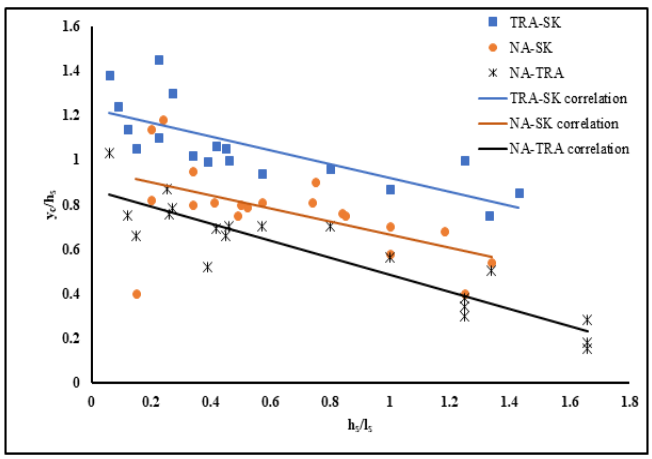


**Figure 2.** Flow regimes over the stepped spillway in the current study

### 3.2 Dissolved oxygen

The flow over the stepped spillway is characterized as a complex and high turbulence flow. The aeration in the free surface adds an extra dimension of complexity to the flow characteristics. To investigate the behaviors of the multiphase flow is needed to obtain the dissolved oxygen concentrations upstream and downstream of the stepped spillway. This section presented the results of chute angle effects and the flow regime on the aeration efficiency E20. Also, the aeration efficiency E20 results were illustrated regarding the stepped spillway geometry and step shapes.

Table 2 shows the impacts of the slope on the Step models of all the groups on the aeration efficiency. Three regimes of flow occur on stepped spillways: (i) Nappe flow at low discharges, (ii) Skimming flow at the high discharges, (iii) and Transition flow in between the Nappe and Skimming flow. Table 2 presents the visual observations of the flow regimes with the flat step models. In group one for M1-1 and M1-4 models with the discharge (Q) of $4.35 \times 10^{-3}$ $m^3$/sec, the observations showed a Nappe flow regime for M1-1 and M1-4 models with E20 = 42.87% and 44.16% respectively. In other hand, the Transition flow regimes observed with discharge $Q = 10.10 \times 10^{-3}$ $m^3$/sec when E20 = 38.55% at M1-1 model and E20 = 39.06% at M1-4 model. For both models (M1-1 and M1-4), the Skimming flow regimes observed with discharge $Q = 38.46 \times 10^{-3}$ $m^3$/sec and E20 = 22.02% and 23.17% respectively. The results show the aeration efficiency changed with the flow regime type. From Table 2, the flat step models in groups two and three have the same behaviors except for the aeration efficiency increased with increasing the step length and decreasing the chute angle for the same discharges. According to the differences in aeration mechanisms in the flow regimes, the aeration efficiency in the flow regimes has differed significantly from each other. The results show that when the discharge is low with the Nappe flow regime leads to high aeration efficiency than the other flow regimes. In the low discharges with the Nappe flow regime, the high aeration efficiency may come from the Nappe flow regime characteristics, the long residence time, and large air bubbles entrainment. However, the lowest aeration efficiency was clear at the high discharges with the Skimming flow regime and increasing the chute angle because the high velocity of the flow leads to a decrease in the residence time, and maybe there is small air bubbles entrainment.

Tables 3 and 4 present the results of the other step shapes in all the groups to determine the slope effect on the aeration efficiency. The result shows that as the chute angle decreases, the aeration efficiency increases for the same discharge. Moreover, $E_{20}$ increased with the flow over the new step shape (step with quarter-circle end sill) more than in other step shapes. The highest $E_{20}$ has been achieved in M3-3 for $Q = 4.35 \times 10^{-3}$ $m^3$/s for $\theta = 8.9°$. The difference in $E_{20}$ = 21.49% between M3-3 and M1-1 because of the slope and the step shape effects. This development in the performance of the stepped spillway with the new step shape (step with quarter-circle end sill) highlighted the positive contribution with respect to $E_{20}$.

Figure 3 demonstrates the aeration efficiency of E20 in all groups with all the step configurations that have step height hs = 0.03 m and hs = 0.05 m with non-dimensional yc/hs for discharge range 4.35 × 10-3 to 55.56 × 10-3 m3/sec. In group one, for the M1-1 and M1-4 models, the yc/hs = 0.66 and 0.40 with the maximum E20 = 44.16 % and 42.87% respectively.

For the same values for yc/hs with normal end sill models, M1-2 and M1-5 models the maximum E20 = 51.21% and 48.22% respectively, meanwhile at M1-3 and M1-6 models the maximum E20 = 53.10% and 49.02% as shown in Figures 3.1a, 3.1b, and 3.1c illustrated the E20 on groups two and three and showed the same behavers for group one. The high aeration efficiency E20 was in the M3-3 model in group three when compared with others. When the chute angle changed from 26.6° to 8.9°, the aeration efficiency E20 improved with 11.51% at the lowest discharge and 6.05% at the highest discharge for the M1-1 model. Also, E20 improved with 11.39% at the lowest discharge and 6.50% at the highest discharge for the M1-4 model. The aeration efficiency increases with decreasing the chute angle. The main reason for the aeration efficiency increasing overstepped spillway when the chute angle decrease, for constant spillway height $H_d$, is coming from the increase in the number of the step Ns, and step length ls which leads to increase the residence time.

Figure 4 presented the aeration efficiency E20 as a function of energy dissipation ΔE/Eo for all the step configurations in the current study. The data showed a power Equation relationship as follows:

$$E_{20} = 0.0096 \times \left(\frac{\Delta E}{E_o}\right)^{1.915} \quad (R^2 = 0.91) \quad \text{for Groups one and two} \tag{10}$$

$$E_{20} = 0.0109 \times \left(\frac{\Delta E}{E_o}\right)^{1.927} \quad (R^2 = 0.94) \quad \text{for Group three} \tag{11}$$

where, $R^2$ is the correlation coefficient.

**Table 2.** Measured aeration efficiency versus chute angles with flat step shape

| Q ×10$^{-3}$ (m$^3$/s) | θ | M 1-1, group 1, $N_s$ = 10 steps | | M 1-4, group 1, $N_s$ = 6 steps | |
|---|---|---|---|---|---|
| | | $E_{20}$ % | Flow regime | $E_{20}$ % | Flow regime |
| 4.35 | 26.6° | 44.16 | Nappe | 42.87 | Nappe |
| 10.10 | 26.6° | 39.06 | Transition | 38.55 | Transition |
| 25.00 | 26.6° | 30.27 | Transition | 29.48 | Transition |
| 38.46 | 26.6° | 23.17 | Skimming | 22.02 | Skimming |
| 55.56 | 26.6° | 21.03 | Skimming | 19.89 | Skimming |
| Q ×10$^{-3}$ (m$^3$/s) | θ | M 2-1, group 2, $N_s$ = 10 steps | | M 2-4, group 2, $N_s$ = 6 steps | |
| | | $E_{20}$ % | Flow regime | $E_{20}$ % | Flow regime |
| 4.35 | 21.8° | 46.38 | Nappe | 44.32 | Nappe |
| 10.10 | 21.8° | 40.30 | Transition | 38.98 | Transition |
| 25.00 | 21.8° | 33.03 | Transition | 31.13 | Transition |
| 38.46 | 21.8° | 28.12 | Skimming | 26.11 | Skimming |
| 55.56 | 21.8° | 21.19 | Skimming | 20.29 | Skimming |
| Q ×10$^{-3}$ (m$^3$/s) | θ | M 3-1, group 3, $N_s$ = 10 steps | | M 3-4, group 3, $N_s$ = 6 steps | |
| | | $E_{20}$ % | Flow regime | $E_{20}$ % | Flow regime |
| 4.35 | 8.9° | 55.67 | Nappe | 54.26 | Nappe |
| 10.10 | 8.9° | 51.28 | Nappe | 49.72 | Nappe |
| 25.00 | 8.9° | 44.36 | Transition | 42.00 | Transition |
| 38.46 | 8.9° | 36.72 | Skimming | 34.09 | Skimming |
| 55.56 | 8.9° | 27.08 | Skimming | 26.39 | Skimming |

**Table 3.** Measured aeration efficiency versus chute angles with normal end sill step shape

| Q ×10$^{-3}$ (m$^3$/s) | θ | M 1-2, group 1, $N_s$ = 10 steps | | M 1-5, group 1, $N_s$ = 6 steps | |
|---|---|---|---|---|---|
| | | $E_{20}$ % | Flow regime | $E_{20}$ % | Flow regime |
| 4.35 | 26.6° | 51.21 | Nappe | 48.22 | Nappe |
| 10.10 | 26.6° | 45.23 | Nappe | 42.14 | Transition |
| 25.00 | 26.6° | 39.25 | Transition | 35.04 | Transition |
| 38.46 | 26.6° | 30.08 | Skimming | 28.20 | Skimming |
| 55.56 | 26.6° | 24.27 | Skimming | 22.30 | Skimming |
| Q ×10$^{-3}$ (m$^3$/s) | θ | M 2-2, group 2, $N_s$ = 10 steps | | M 2-5, group 2, $N_s$ = 6 steps | |
| | | $E_{20}$ % | Flow regime | $E_{20}$ % | Flow regime |
| 4.35 | 21.8° | 53.11 | Nappe | 50.14 | Nappe |
| 10.10 | 21.8° | 47.85 | Nappe | 44.22 | Nappe |
| 25.00 | 21.8° | 40.20 | Transition | 37.08 | Transition |
| 38.46 | 21.8° | 33.18 | Skimming | 30.52 | Skimming |
| 55.56 | 21.8° | 25.37 | Skimming | 23.15 | Skimming |
| Q ×10$^{-3}$ (m$^3$/s) | θ | M 3-2, group 3, $N_s$ = 10 steps | | M 3-5, group 3, $N_s$ = 6 steps | |
| | | $E_{20}$ % | Flow regime | $E_{20}$ % | Flow regime |
| 4.35 | 8.9° | 62.95 | Nappe | 59.95 | Nappe |
| 10.10 | 8.9° | 58.36 | Nappe | 53.95 | Nappe |
| 25.00 | 8.9° | 52.39 | Transition | 49.96 | Transition |
| 38.46 | 8.9° | 41.45 | Transition | 39.32 | Skimming |
| 55.56 | 8.9° | 31.06 | Skimming | 29.54 | Skimming |

**Table 4.** Measured aeration efficiency versus chute angles with the quarter-circle end sill step shape

| Q ×10$^{-3}$ (m$^3$/s) | θ | M 1-2, group 1, $N_s$ = 10 steps | | M 1-5, group 1, $N_s$ = 6 steps | |
|---|---|---|---|---|---|
| | | $E_{20}$ % | Flow regime | $E_{20}$ % | Flow regime |
| 4.35 | 26.6° | 53.10 | Nappe | 49.02 | Nappe |
| 10.10 | 26.6° | 48.12 | Nappe | 43.98 | Nappe |
| 25.00 | 26.6° | 40.10 | Transition | 38.42 | Transition |
| 38.46 | 26.6° | 30.52 | Transition | 29.02 | Skimming |
| 55.56 | 26.6° | 25.21 | Skimming | 23.15 | Skimming |
| Q ×10$^{-3}$ (m$^3$/s) | θ | M 2-2, group 2, $N_s$ = 10 steps | | M 2-5, group 2, $N_s$ = 6 steps | |
| | | $E_{20}$ % | Flow regime | $E_{20}$ % | Flow regime |
| 4.35 | 21.8° | 55.63 | Nappe | 51.10 | Nappe |
| 10.10 | 21.8° | 50.57 | Nappe | 46.11 | Nappe |
| 25.00 | 21.8° | 43.02 | Transition | 39.23 | Transition |
| 38.46 | 21.8° | 34.12 | Transition | 31.45 | Transition |
| 55.56 | 21.8° | 26.08 | Skimming | 24.06 | Skimming |
| Q ×10$^{-3}$ (m$^3$/s) | θ | M 3-2, group 3, $N_s$ = 10 steps | | M 3-5, group 3, $N_s$ = 6 steps | |
| | | $E_{20}$ % | Flow regime | $E_{20}$ % | Flow regime |
| 4.35 | 8.9° | 65.65 | Nappe | 62.30 | Nappe |
| 10.10 | 8.9° | 59.99 | Nappe | 56.42 | Nappe |
| 25.00 | 8.9° | 53.85 | Nappe | 52.57 | Transition |
| 38.46 | 8.9° | 42.67 | Transition | 40.91 | Transition |
| 55.56 | 8.9° | 32.90 | Skimming | 30.65 | Skimming |

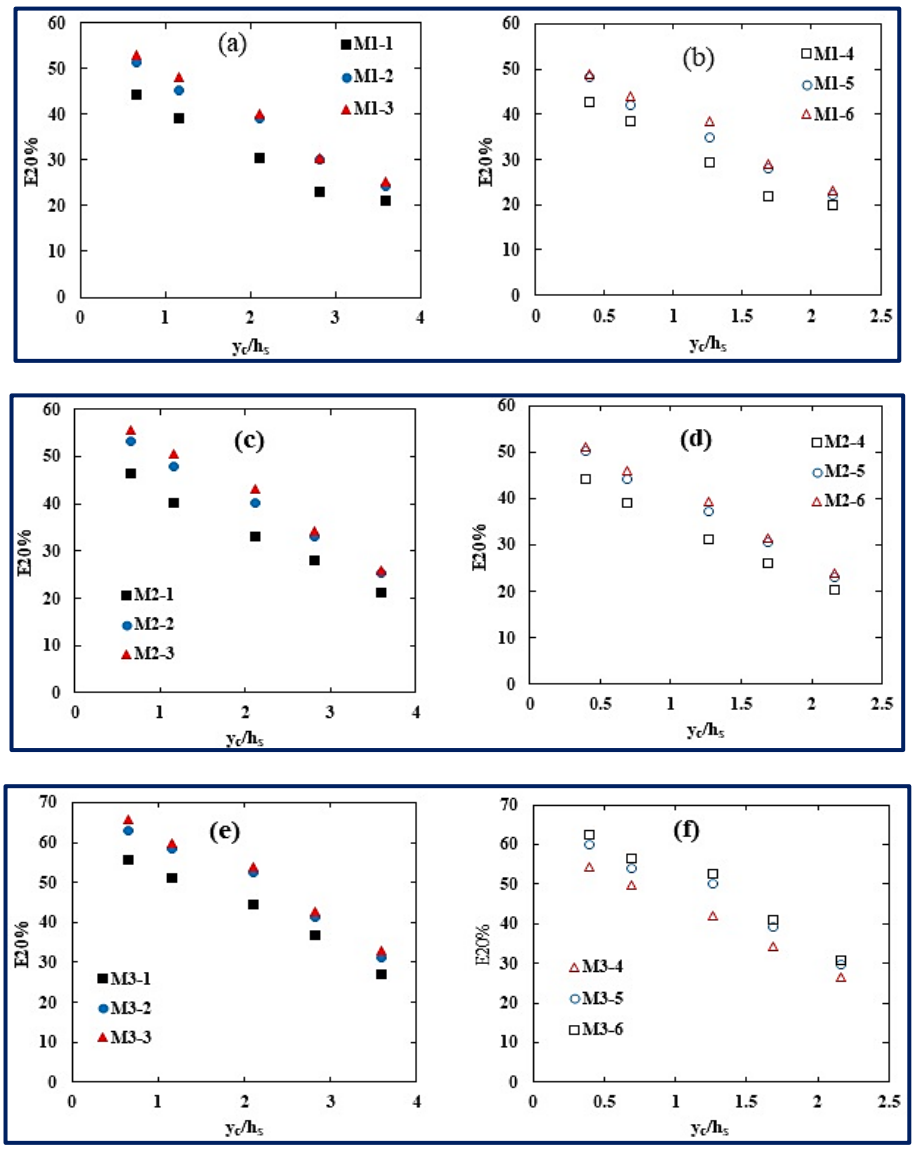


**Figure 3.** Aeration efficiency in various the step configurations, (a): group-1 for hs= 3 cm, (b): group-1 for hs= 5 cm, (c): group-2 for hs= 3 cm, (d): group-2 for hs= 5 cm, (e): group-3 for hs= 3 cm, (f): group-3 for hs= 5 cm

The proposed Eqns. (10) & (11) are valid within the range of the present study including q ranging from $9 \times 10^{-3}$ $m^3/s$. m to a maximum of $111 \times 10^{-3}$ $m^3/s$. m, for step height hs = 3 cm and 5 cm.

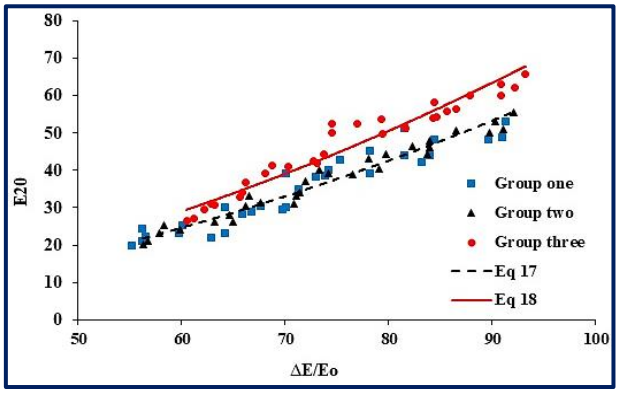


**Figure 4.** Aeration efficiency with energy dissipation at the downstream end of the stepped spillway for all tested configurations

### 3.3 The inception points of free surface

At the end of the upstream for the stepped spillway, the surface of the flow was smooth, and some small waves developed. When the small waves started to break down the free surface changed to berserk and rough. The changes in the free surface properties happened fast across the flow width and this phenomenon is called the inception point as shown in Figure 5. The inception point phenomena were important to obtain a good understanding of the effects of micro-roughness on the free surface and aeration.

**Figure 5.** Free-surface aeration on stepped spillway (M1-3)

Figures 6, 7, and 8 presented the relationship between the inception point location (where: Li is the length from the upstream crest to the inception point of free-surface self-aeration, and ks is the step roughness height) and the Froude number defined in terms of roughness height Fr*. For all stepped spillway models, the locations of the inception point of aeration were recorded for $0.9 < yc/hs < 1.7$ and $0.9 < yc/hs < 1.7$ for hs = 0.03 m and hs = 0.05 m respectively.

The inception point locations of the free-surface aeration were noted by some detailed visual observations, and there were small changes in the same group as shown in comparison in Figures 6, 7, and 8. In all the steps configurations, at low discharges with low Fr* the inception point location Li was low with a little variation. However, at high discharge with high Fr* the inception point location Li was longer with a high variation. M1-3 and M1-6 models have lower Li/ks values when compared with the rest of the models because of the effect of the semi-circle shape for the end sill. In general, when the discharge increases led to an increase in both length of inception point location Li and Froude roughness number Fr*. Groups two and three have different behavers for the M1-3 and M1-6 models because the values of Li were close to the other models as shown in Figures 7 and 8.

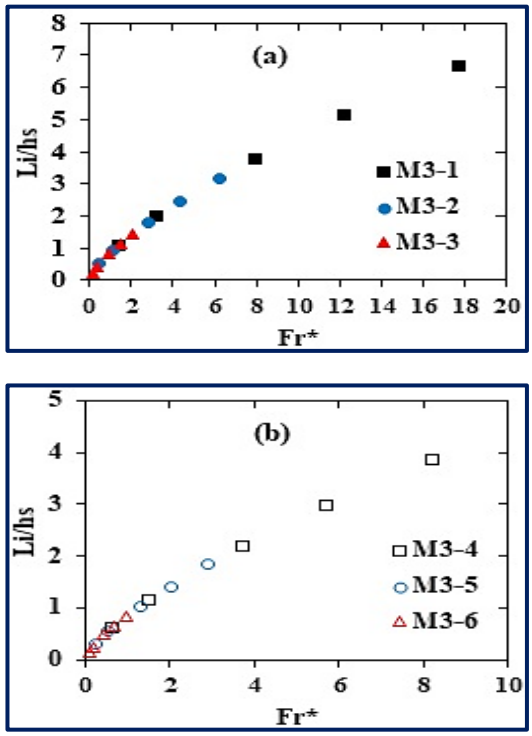


**Figure 6.** Locations of the inception point of group one (a): Models with hs = 3 cm, (b): Models with hs = 5 cm

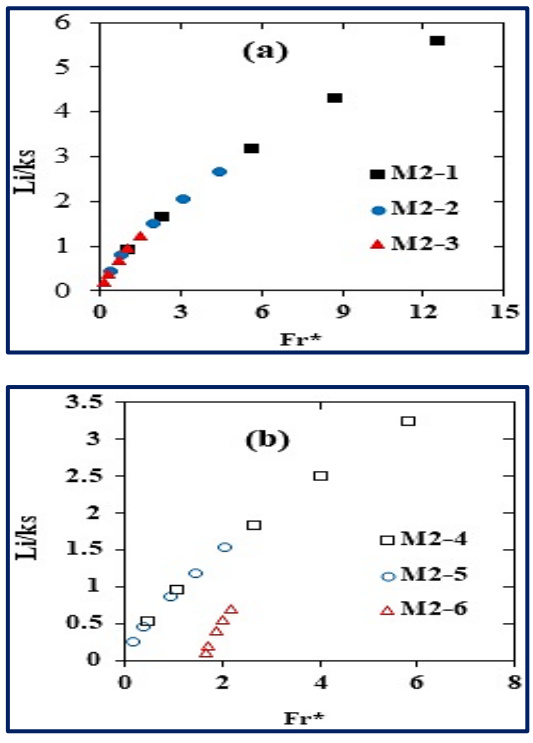


**Figure 7.** Locations of the inception point of group two (a): Models with hs = 3 cm, (b): Models with hs = 5 cm

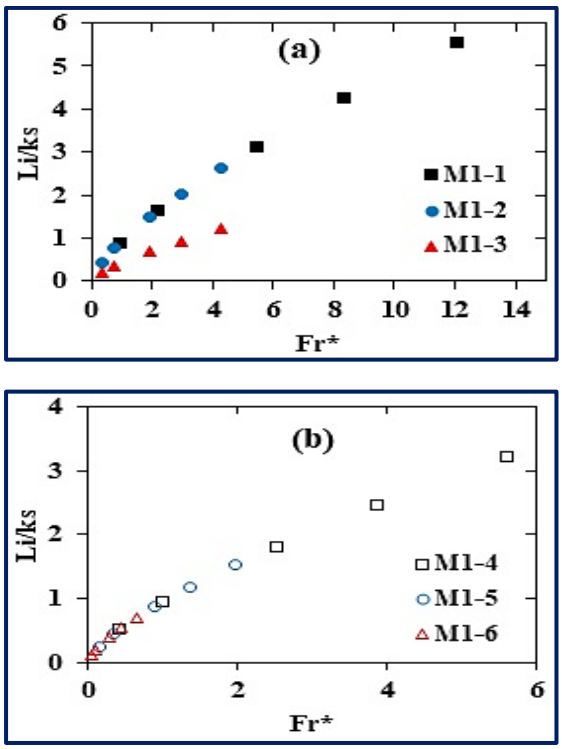


**Figure 8.** Locations of the inception point of group three (a): Models with hs = 3 cm, (b): Models with hs = 5 cm

The relationship between the inception point location (where, Li is the length from the upstream crest to the inception point of free-surface self-aeration, and $k_s$ is the step roughness height) and the Froude number defined in terms of roughness height Fr* can be presented by Eqns. (12)-(14).

$$Li/Ks = 0.938 \times (Fr*)^{0.713} \quad (R^2 = 0.98) \quad (12)$$

$$Li/Ks = 0.924 \times (Fr*)^{0.721} \quad (R^2 = 0.99) \quad (13)$$

$$Li/Ks = 0.862 \times (Fr*)^{0.736} \quad (R^2 = 0.97) \quad (14)$$

### 3.4 Water surface profile above the crest

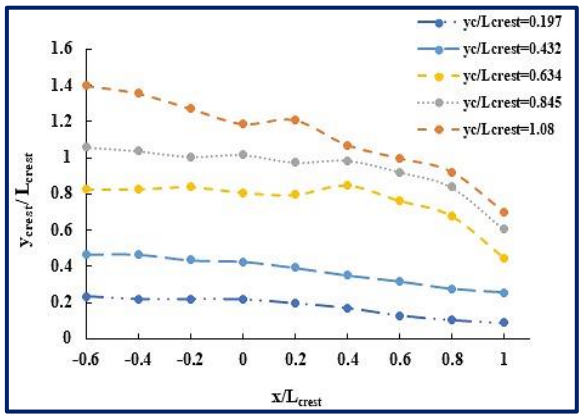


**Figure 9.** Water surface profile over the crest for stepped spillway at the M1-1

The water surface profile depths were measured before and at the crest (Lcrest = 0.1 m) was the length of the crest) on nine locations (- 0.6 ≤ X / Lcrest ≤ 1) by using the pointer gauge for five discharges (yc/Lcrest = 0.197, 0.432, 0.634, 0.845, and 1.08).

where, x is the horizontal distance and yc was the critical flow depth. Figure 9 presented the non-dimensional free surface profile for the M1-1 model with chute angle Θ = 26.6° as an example. Photographs of discharges above the crest of the stepped spillway were shown in Figure 10. At low discharges (yc/Lcrest ≤ 0.432), the surface profile of the water showed very small waves which were close to the smooth shape with subcritical flow above most of the crest. The smooth water surface came as a result of the energy losses and the developed boundary layer impacts [20, 21]. Figure 10 showed the free surface of the water at high discharges (yc/Lcrest ≥ 0.432). The free surface of water fell continuously with the flow direction.

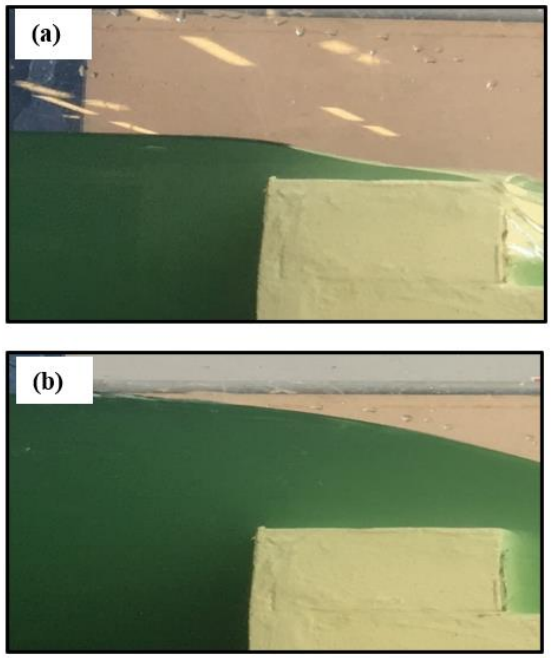


**Figure 10.** Water-free surface over the crest for M1-1, (a): yc/Lcrest ≤ 0.432, (b): yc/Lcrest ≥ 0.432

## 4. CONCLUSIONS

Hydraulic structures were created to increase the dissolved oxygen by generating turbulent conditions where small air bubbles are carried into the bulk of the flow. The current study provides an experimental and numerical investigation of the aeration efficiency and flow regimes of the overstepped spillway with different chute angles, step shapes, and step heights. The following conclusions can be deduced from the study:

1. The aeration efficiency significantly changes depending on the flow conditions and that comes from the different mechanisms of air entrainment in the flow regimes (nappe, transition, and skimming flow).
2. At low discharge with nappe flow regime, the aeration efficiency is high when compared with the high discharge with transition and skimming flow regimes and that means when the discharge increase leads to a decrease in the aeration efficiency.
3. The stepped geometry has the main impact on the aeration process and that is clear in the pooled step shape.
4. From the results, when the chute angle increases the aeration efficiency decrease at any discharge.

## ACKNOWLEDGMENT

The authors would like to thank all the staff of the Digital Manufacturing and Civil Laboratories at Deakin University for their assistance and support. Lulea university of technology-Sweden and Al-Mustaqbal University College-Iraq supported the authors by the fund.

## REFERENCES

[1] Cox, B.A. (2003). A review of dissolved oxygen modelling techniques for lowland rivers. Science of the Total Environment, 314: 303-334. https://doi.org/10.1016/S0048-9697(03)00062-7

[2] Toombes, L. (2002). Experimental study of air-water flow properties on low-gradient stepped cascades. Department of Civil Engineering, Faculty of Engineering, Physical Sciences and Architecture, The University of Queensland, Brisbane, Australia. https://core.ac.uk/download/pdf/14982737.pdf, accessed on March 17, 2014.

[3] Baylar, A., Bagatur, T. (2000). Aeration performance of weirs. Water Sa, 26(4): 521-526.

[4] Bagatur, T. (2009). Evaluation of preparation with V-Notch Weir and cascade structures in clarifiers. Journal of Environmental Engineering, 135(3): 176-184. https://doi.org/10.1061/(ASCE)0733-9372(2009)135:3(176)

[5] Wang, H., Bai, Z.T., Bai, R.D., Liu, S.J. (2022). Self-aeration of supercritical water flow rushing down artificial vegetated stepped chutes. Water Resources Research, p. e2021WR031719. https://doi.org/10.1029/2021WR031719

[6] Ashour, M.A., Aly, T.E., Ali, M.K. (2019). An investigation concerning the water energy dissipation and flow aeration over stepped spillways. In 22 International Water Technology Conference, IWTC22, Ismailia, pp. 478-489.

[7] Felder, S., Geuzaine, M., Dewals, B., Erpicum, S. (2019). Nappe flows on a stepped chute with prototype-scale steps height: Observations of flow patterns, air-water flow properties, energy dissipation and dissolved oxygen. Journal of Hydro-environment Research, 27: 1-19. https://doi.org/10.1016/j.jher.2019.07.004

[8] Wan, W., Raza, A., Chen, X. (2019). Effect of height and Geometry of stepped spillway on inception point location. Applied Sciences, 9(10): 2091. http://dx.doi.org/10.3390/app9102091

[9] Chanson, H. (1997). Air bubble entrainment in open channels: Flow structure and bubble size distributions. International Journal of Multiphase Flow, 23(1): 193-203. https://doi.org/10.1016/S0301-9322(96)00063-8

[10] Baylar, A., Emiroglu, M., Bagatur, T. (2009). Influence of chute slope on oxygen content in stepped waterways. Gazi University Journal of Science, 22(4): 325-332.

[11] Baylar, A., Unsal, M., Ozkan, F. (2011). The effect of flow patterns and energy dissipation over stepped chutes on aeration efficiency. KSCE Journal of Civil Engineering, 15(8): 1329-1334. https://doi.org/10.1007/s12205-011-1360-0

[12] Bung, D.B. (2011). Developing flow in skimming flow regime on embankment stepped spillways. Journal of Hydraulic Research, 49(5): 639-648. https://doi.org/10.1080/00221686.2011.584372

[13] Zare, H.K., Doering, J.C. (2012). Effect of rounding edges of stepped spillways on the flow characteristics. Canadian Journal of Civil Engineering, 39(2): 140-153. https://doi.org/10.1139/l11-121

[14] Felder, S., Chanson, H. (2013). Aeration, flow instabilities, and residual energy on pooled stepped spillways of embankment dams. Journal of Irrigation and Drainage Engineering, 139(10): 880-887. https://doi.org/10.1061/(ASCE)IR.1943-4774.0000627

[15] Felder, S., Chanson, H. (2013). Air–water flow measurements in a flat slope pooled stepped waterway. Canadian journal of civil engineering, 40(4): 361-372. https://doi.org/10.1139/cjce-2012-0464

[16] Gulliver, J.S., Thene, J.R., Rindels, A.J. (1990). Indexing gas transfer in self-aerated flows. Journal of Environmental Engineering. 116(3): 503-523. https://doi.org/10.1061/(ASCE)0733-9372(1991)117:6(867.2)

[17] Ozkan, F., Tuna, M.C., Baylar, A., Ozturk, M. (2014). Optimum air-demand ratio for maximum aeration efficiency in high-head gated circular conduits. Water Science and Technology, 70(5): 871-877. http://dx.doi.org/10.2166/wst.2014.305

[18] Carosi, G., Chanson, H. (2008). Turbulence characteristics in skimming flows on stepped spillways. Canadian Journal of Civil Engineering, 35(9): 865-880. https://doi.org/10.1139/L08-030

[19] Chanson, H., Toombes, L. (2004). Hydraulics of stepped chutes: The transition flow. Journal of Hydraulic Research. 42(1): 43-54. https://doi.org/10.1080/00221686.2004.9641182

[20] Chanson, H. (2001). Hydraulic design of stepped spillways and downstream energy dissipators. Dam Engineering, 11(4): 205-242.

[21] Isaacs, L.T. (1981). Effects of laminar boundary layer on a model broad-crested weir. Research Report No. CE28, Dept. of Civil Eng., The Univ. of Queensland, Brisbane, Australia, p. 20.

## NOMENCLATURE

| | |
|---|---|
| Dc/dt | rate of change in concentration |
| A | the surface area of bubbles |
| ∀ | the volume of water in which the C and A are measured |
| C | the DO concentration in water |
| CS | the saturation concentration of oxygen in the water |
| kL | the liquid film coefficient |
| t | the time |
| Cu | the dissolved oxygen concentration upstream of the hydraulic structure |
| Cd | dissolved oxygen concentration downstream of the hydraulic structure |
| E | the actual aeration efficiency |
| E20 | the aeration efficiency at 20℃ and ft is the exponent described by Eq. (4) |
| T | the water temperature |
| Li | the non-aerated flow region length |
| ws | the sill height |

| | | | |
|---|---|---|---|
| F* | the Froude number and is defined in terms of the step cavity roughness | ls | the step length |
| | | $L_{crest}$ | the length of the crest |
| $y_c$ | the critical flow depth | Θ | the chute angle |
| hs | the step height | Hd | the weir depth |